

The effect of pressure and alloying on half-metallicity of quaternary Heusler compounds CoMnYZ ($Z = \text{Al, Ga, and In}$)

M. RAHMOUNE^{1,*}, A. CHAHED¹, A. AMAR¹, H. ROZALE¹, A. LAKDJA¹, O. BENHELAL¹, A. SAYEDE²

¹Condensed Matter and Sustainable Development Laboratory, University of Sidi Bel-Abbes, Sidi Bel-Abbes 22000, Algeria

²UCCS, CNRS-UMR 8181, Université d'Artois, Faculté des Sciences Jean Perrin, Rue Jean Souvraz, SP 18, 62307 Lens Cedex, France

In this work, first-principles calculations of the structural, electronic and magnetic properties of Heusler alloys CoMnYAl , CoMnYGa and CoMnYIn are presented. The full potential linearized augmented plane waves (FP-LAPW) method based on the density functional theory (DFT) has been applied. The structural results showed that CoMnYZ ($Z = \text{Al, Ga, In}$) compounds in the stable structure of type 1+FM were true half-metallic (HM) ferromagnets. The minority (half-metallic) band gaps were found to be 0.51 (0.158), 0.59 (0.294), and 0.54 (0.195) eV for $Z = \text{Al, Ga, and In}$, respectively. The characteristics of energy bands and origin of minority band gaps were also studied. In addition, the effect of volumetric and tetragonal strain on HM character was studied. We also investigated the structural, electronic and magnetic properties of the doped Heusler alloys $\text{CoMnYGa}_{1-x}\text{Al}_x$, $\text{CoMnYAl}_{1-x}\text{In}_x$ and $\text{CoMnYGa}_{1-x}\text{In}_x$ ($x = 0, 0.25, 0.5, 0.75, 1$). The composition dependence of the lattice parameters obeys Vegard's law. All alloy compositions exhibit HM ferromagnetic behavior with a high Curie temperature (T_C).

Keywords: *density functional theory; quaternary Heusler compounds; half-metallic ferromagnetic; magnetism*

© Wrocław University of Technology.

1. Introduction

As is known, searching for semiconductor with half-metallic (HM) ferromagnetism is of importance for the development of spintronics. Since the half-Heusler alloy NiMnSb was firstly predicted to be a half-metallic ferromagnet (HFM) by utilizing the first principles calculations in 1983 [1], new half-metallic Heusler alloys, which are metallic for one spin direction while semiconducting for the other spin direction, have always received the theoretical and experimental attention due to their potential applications in the fields of magnetic sensors, tunnel junctions and other spintronic devices [2–4]. Heusler alloys, with structural formulas of X_2YZ (with L2_1 structure) and XYZ (with Cl_b structure), in which X and Y are transition

metals and Z is a main-group element, are one of the most attractive HM materials, since they can be synthesized easily and their Curie temperatures are high [5–9]. Recently, another family of Heusler compounds known as quaternary Heusler alloys with chemical formula of XX'YZ (X, X', and Y are transition metals, and Z is a main-group element) have been considered. XX'YZ quaternary Heusler compounds crystallize in the LiMgPdSn -type crystal structure [10, 11] with F43m symmetry. In these compounds, the atomic number of X' is usually lower than the valence of X atoms, and the atomic number of the Y element is lower than that of both X and X'. A variety of new research related to quaternary Heusler alloys shows that they exhibit HMF [12–16]. Felser's research group [10, 17–19] theoretically predicted HM ferromagnetism in several quaternary Heusler compounds such as CoFeMnZ ($Z = \text{Al, Si, Ga, Ge}$), NiFeMnGa , and

*E-mail: rahmounemohammed@yahoo.fr

NiCoMnGa. They also synthesized successfully these compounds and observed high Curie temperatures (from 326 K to 711 K) [17, 19]. Compared with the pseudoternary Heusler half-metals, quaternary ones with a 1:1:1:1 stoichiometry have the advantage of lower-power dissipation due to the slight disorder in them [19, 20].

Yet quaternary Heusler compounds with interesting properties have not been investigated. In order to further design and develop novel quaternary Heusler compounds to meet the demands of spintronics, we have used *ab initio* electronic-structure calculations to identify these interesting compounds for spintronics applications. In the current work, we present the results of structural, electronic and magnetic properties of the novel quaternary half-metallic Heusler alloys CoMnYZ ($Z = \text{Al, Ga, In}$) by using the first-principles calculations. We also discuss the HM stability under hydrostatic strain and tetragonal strain.

Finally, the effect of the substitution of Z sp atoms on the structural, electronic and magnetic properties of CoMnYGa $_{1-x}$ Al $_x$, CoMnYGa $_{1-x}$ In $_x$ and CoMnYAl $_{1-x}$ In $_x$ Heusler alloys is presented. To the best of our knowledge, these quaternary Heusler compounds are actually the first reported up to now. This paper is organized as follows: Section 2 presents the details of calculations. Section 3 contains the results and discussion and Section 4 summarizes the main results.

2. Computational method

We have carried out first-principles calculations [21] with both full potential and linear augmented plane wave (FP-LAPW) method [22] as implemented in the WIEN2k code [23]. We have adopted the generalized gradient approximation (GGA) in the scheme of Perdew-Burke-Ernzerhof (PBE) [24]. In the calculations reported here, we use a parameter $R_{\text{MT}}K_{\text{max}} = 9$, which determines matrix size (convergence), where K_{max} is the plane wave cut-off and R_{MT} is the smallest of all atomic sphere radii. We have chosen the muffin-tin radii (MT) for Co, Mn, Y, Al, Ga and In to be 2.35, 2.35, 2.35, 2.1, 2.35 and 2.45 a.u., respectively. Within

these spheres, the charge density and potential are expanded in terms of crystal harmonics up to angular momenta $L = 10$, and a plane wave expansion is used in the interstitial region. The value of $G_{\text{max}} = 14$, where G_{max} is defined as the magnitude of largest vector in charge density Fourier expansion. The Monkhorst-Pack special k-points were performed using 8000 special k-points in the Brillouin zone. The cutoff energy, which defines the separation of valence and core states, was chosen as -6 Ry. The charge convergence of 0.0001 e has been selected during self-consistency cycles.

3. Results and discussion

3.1. Structural properties

The structural prototype of the quaternary Heusler compounds – LiMgPdSb – is denoted as Y [10]. There are three possible different types of atom arrangement in the quaternary Heusler compound $XX'YZ$: Y-type 1: X (0, 0, 0), X' (0.25, 0.25, 0.25), Y (0.5, 0.5, 0.5), and Z(0.75, 0.75, 0.75); Y-type 2: X (0, 0, 0), X' (0.5, 0.5, 0.5), Y(0.25, 0.25, 0.25), and Z (0.75, 0.75, 0.75); Y-type 3: X(0.5, 0.5, 0.5), X' (0, 0, 0), Y (0.25, 0.25, 0.25), and Z (0.75, 0.75, 0.75). In first step, in order to obtain the correct atomic arrangement and the magnetic ground state corresponding to the true ground state of the quaternary Heusler compounds CoMnYZ ($Z = \text{Al, Ga, In}$), we performed the energy minimization as a function of lattice constant with respect to the three different possible site occupation for every non-magnetic (NM), ferromagnetic (FM) and antiferromagnetic (AFM) configurations and the obtained curves are shown in Fig. 1 and Fig. 2. The calculated total energies within GGA as a function of volume are fitted to Murnaghan's equation of state to obtain the ground-state properties [25]. In Table 1, there are presented our calculated equilibrium lattice constant a_0 , along with the bulk modulus B_0 , and the total energy E_{tot} in their different structural and magnetic configurations. As seen in Fig. 1 and Fig. 2, the optimization of the cubic lattice parameters for all three possible configurations in their respective three

different magnetic configurations reveal the lowest energy for Y-type 1 structure with a ferromagnetic ground state for all compounds. In the absence of the experimental data regarding the lattice constant a_0 and bulk modulus B_0 , the parameters of the material of interest, and hence our results are predictions. Also, the highest calculated bulk moduli for CoMnYZ ($Z = \text{Al, Ga, In}$) in Y-type 1+FM configuration confirm the stability of this structure. In the same way, the formation energy E_f determines whether a compound can be experimentally synthesized or not. E_f is the change in energy when a material is formed from its constituent elements in their bulk states and can be calculated for CoMnYZ ($Z = \text{Al, Ga, In}$) compounds as:

$$E_f^{\text{CoMnYZ}} = E_{\text{tot}}^{\text{CoMnYZ}} + (E_{\text{Co}}^{\text{bulk}} + E_{\text{Mn}}^{\text{bulk}} + E_{\text{Y}}^{\text{bulk}} + E_{\text{Z}}^{\text{bulk}}) \quad (1)$$

$Z = \text{Al, Ga, In}$

where $E_{\text{tot}}^{\text{CoMnYZ}}$ are the first-principles calculated equilibrium total energies of studied compounds per formula unit, $E_{\text{Co}}^{\text{bulk}}$, $E_{\text{Mn}}^{\text{bulk}}$, $E_{\text{Y}}^{\text{bulk}}$ and $E_{\text{Z}}^{\text{bulk}}$ are the calculated equilibrium total energies of these atoms in their stable bulk phases. In Table 1, there are given the values of formation energy for all types of structures and all magnetic configurations. These values imply that the three compounds can be fabricated spontaneously in experiment due to their negative formation energy. Also, according to Table 1, the calculated E_f values confirm the structural stability of type1+FM structure for all CoMnYZ ($Z = \text{Al, Ga, In}$) compounds (high negative formation energy). Among them, CoMnYAl is most easily synthesized because of its lowest formation energy. Based on this, all the further calculations on electronic and magnetic properties of CoMnYZ ($Z = \text{Al, Ga, In}$) were performed on this structure only, i.e. in the type 1+FM structure.

3.2. Electronic and magnetic properties

The spin-polarized band structures of ferromagnetic CoMnYZ ($Z = \text{Al, Ga, In}$) at equilibrium lattice constants are shown in Fig. 3. The Fermi level is set as 0 eV. For these compounds, the minority-spin channel is metallic whereas in the majority-spin channel there is an energy gap around the Fermi level. Its value, listed

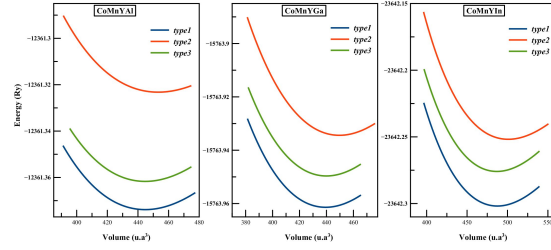


Fig. 1. Total energy as a function of volume per formula unit (f.u.) in the three atomic arrangements: type 1, type 2 and type 3 for the CoMnYZ ($Z = \text{Al, Ga, and In}$) compounds. The curves correspond to the FM state.

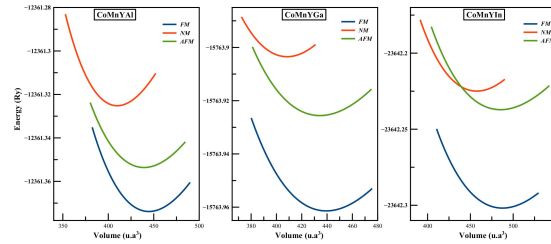


Fig. 2. Total energy as a function of volume per formula unit (f.u.) in the three magnetic states FM, AFM and NM for the CoMnYZ ($Z = \text{Al, Ga, and In}$) compounds. The curves correspond to the type 1 structure.

in Table 2, is about 0.51 eV, 0.59 eV and 0.54 eV for CoMnYAl , CoMnYGa and CoMnYIn , respectively. Therefore, these compounds are HM ferromagnets. The half-metallic gap reported in Table 2, which is determined as the minimum between the lowest energy of majority (minority) spin conduction bands with respect to the Fermi level, and the absolute values of the highest energy of the majority (minority) spin valence bands, are 0.158 eV, 0.294 eV and 0.195 eV, for CoMnYAl , CoMnYGa and CoMnYIn , respectively. On the other hand, the large gaps in these compounds containing localized magnetic orbitals due to d-d hybridization between the transition metal atoms [26] is essential for the gap formation as the p-d hybridization previously discussed [1]. According to Slater-Pauling rule the calculated magnetic moment has to be an integer value for a compound to be a half metal ferromagnet. Indeed, our total magnetic moments

Table 1. Calculated total energies E_{tot} per formula unit, equilibrium lattice constant a_0 , bulk modulus B and formation energy E_f for CoMnYZ ($Z = \text{Al, Ga, In}$) compounds in their different structure types and magnetic configurations.

Compound	Structure	E_{tot} [Ry]			a_0 [Å]	B_0 [GPa]	E_f [Ry]
		NM	FM	AFM			
CoMnYAl	Type 1	-12361.325192	-12361.373842	-12361.353614	6.412	100.212	-1.294
	Type 2	-12361.227488	-12361.323233	-12361.280855	6.453	95.178	-1.243
	Type 3	-12361.325135	-12361.369712	-12361.342789	6.422	102.798	-1.288
CoMnYGa	Type 1	-15763.903474	-15763.961374	-15763.925582	6.387	95.621	-1.228
	Type 2	-15763.831806	-15763.934409	-15763.854632	6.436	93.368	-1.142
	Type 3	-15763.903455	-15763.949612	-15763.925582	6.389	98.016	-1.189
CoMnYIn	Type 1	-23642.224948	-23642.301847	-23642.237173	6.613	92.844	-1.168
	Type 2	-23642.137606	-23642.251825	-23642.185687	6.672	83.238	-1.101
	Type 3	-23642.225186	-23642.275945	-23642.275869	6.609	94.409	-1.148

per formula unit reported in Table 2 are found to be integer value $4.00 \mu_B$ for all the compounds, and obey the Slater-Pauling behavior of HM ferromagnets with Heusler structure [27, 28], $M_{\text{tot}} = (Z_{\text{tot}} - 18)$ rather than $M_{\text{tot}} = (Z_{\text{tot}} - 24)$, here M_{tot} and Z_{tot} are the total magnetic moment per formula unit and the number of total valence electrons, respectively. Z_{tot} is 22 for all the CoMnYAl, CoMnYGa and CoMnYIn compounds.

As seen in Table 2, the main contribution to the total magnetic moment is mainly due to transition element (Mn) with little contribution of other transition elements (Co, Y) and the magnetic moments of the Z (Si, Ge, Sn) atoms are quite small. In order to explain the magnetic properties of these compounds and analyse in detail the influence of exchange splitting of the TM-d states, we have calculated the spin-total (spin-TDOS) and partial density of states (spin-PDOS) for the CoMnYAl, CoMnYGa and CoMnYIn compounds presented in Fig. 4, Fig. 5 and Fig. 6, respectively. As it can be seen, the general structure total DOS are similar for our compounds. So, the Fig. 4, Fig. 5 and Fig. 6 confirm that the main contribution to the magnetic moment of the transition elements (Co, Mn, Y) is due to d states and that the magnetic moment of the Z atom is due to p states. It can be seen that there is a strong hybridization between Co, Mn, and Y atoms, which splits the d orbitals of these atoms into bonding e_g and t_{2g} orbitals (below the Fermi

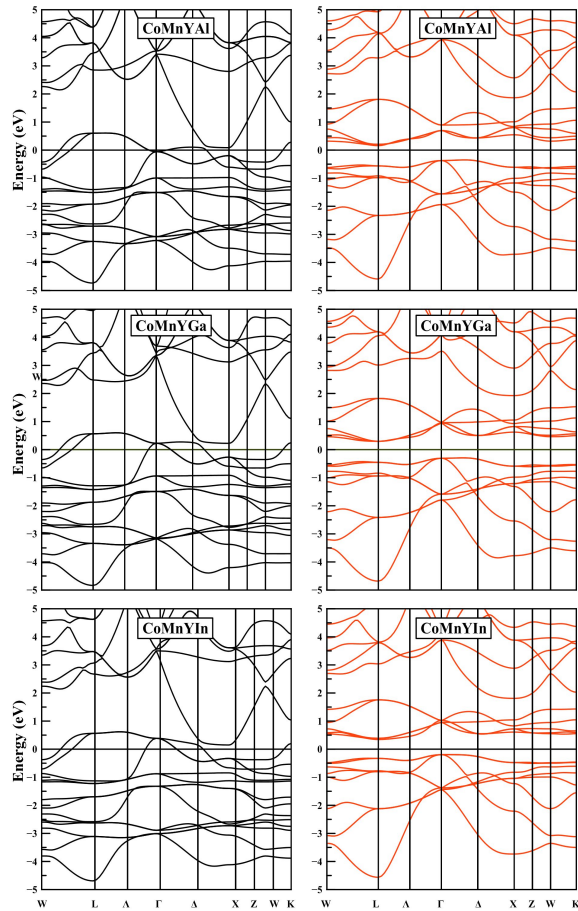


Fig. 3. Spin polarized band structure of CoMnYZ ($Z = \text{Al, Ga and In}$) at their equilibrium lattice constant. The red lines correspond to the majority spin bands (minority spin bands).

Table 2. Semiconducting gap E_g , half-metallic gap E_{HM} , total magnetic moment μ_{tot} , magnetic moment per atom (Co, Mn, Y, Al, Ga, In), magnetic moment in the interstitial region μ_{int} in CoMnYAl, CoMnYGa and CoMnYIn compounds.

Compound	E_g [eV]	E_{HM} [eV]	μ_{tot} [μ_B]	μ_{Co}	μ_{Mn}	μ_Y	μ_X	μ_{int}
CoMnYAl	0.51	0.158	4	0.827	3.5	-0.108	-0.08	-0.139
CoMnYGa	0.59	0.294	4	0.8	3.555	-0.111	-0.072	-0.09
CoMnYIn	0.54	0.195	4	0.75	3.6	-0.137	-0.058	-0.16

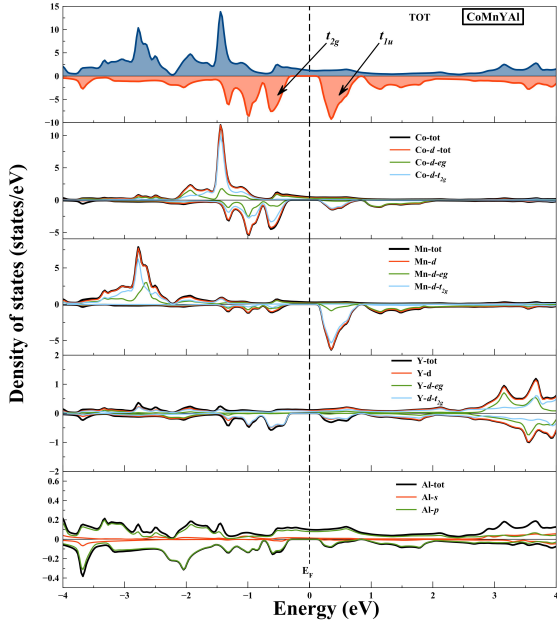


Fig. 4. Spin-polarized total and partial densities of states (DOS) of CoMnYAl.

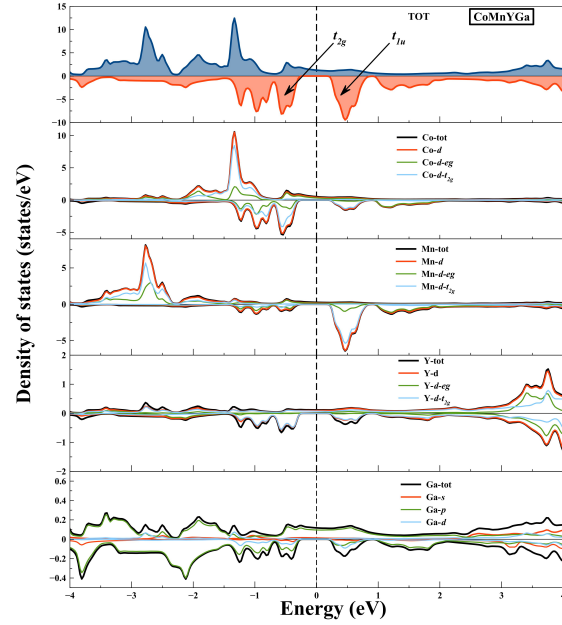


Fig. 5. Spin-polarized total and partial densities of states (DOS) of CoMnYGa.

level), non-bonding e_u and t_{1u} orbitals (around the Fermi level), and anti-bonding e_g and t_{2g} orbitals (above the Fermi level). This hybridization puts the Fermi level in the minority band gap. In fact, d-d hybridization between transition metals takes part in the formation of minority band gap known as d-d band gap. The d-d band gap is the origin of the HM band gap in the full-Heusler alloys with $AlCu_2Mn$ structure [29]. A weaker hybridization is also observed between d states of Co, Mn, and Y atoms with p states of Z atom, which determine the degree of occupation of the p-d orbital. This hybridization affects the width of energy gap.

To illustrate the origin of minority band gap, the orbital hybridization of CoMnYZ is

qualitatively shown in Fig. 7 based on the classical molecular orbital approach. Only the hybridization of d states of Co, Mn and Y atoms has been considered since the sp-bands are located at deep energy and scarcely make contribution to the gap. In the CoMnYZ alloys, the hybridization between Co and Mn is firstly considered since Mn is the first-neighbor atom, as shown in Fig. 7a. The d-orbitals of Co and Mn split into a double degenerate d_{z^2} , $d_{x^2-y^2}$ (noted in Fig. 7 by d_4 , d_5 , respectively) and a triple degenerate d_{xy} , d_{yx} , d_{zx} (noted in Fig. 7 by d_1 , d_2 , d_3 , respectively) orbitals. The double degenerate orbitals d_{z^2} , $d_{x^2-y^2}$ of Co can only couple to the double degenerate orbitals d_{z^2} , $d_{x^2-y^2}$ of Mn forming a bonding orbital e_g and an anti-bonding orbital e_u . The triple degenerate orbitals d_{xy} , d_{yx} , d_{zx} of Co

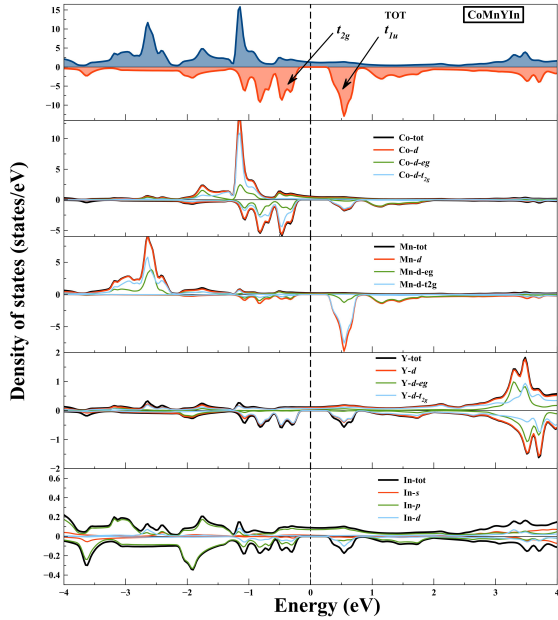


Fig. 6. Spin-polarized total and partial densities of states (DOS) of CoMnYIn.

couple to those of Mn forming a bonding orbital t_{2g} and an anti-bonding orbital t_{1u} . Since the Co and Mn atoms are seated in the center of an octahedron formed by each other, the crystal field splitting of the bonding orbitals is $E(e_g) > E(t_{2g})$ and the anti-bonding orbitals is $E(e_u) > E(t_{1u})$ [3]. Finally, the hybridization of Co–Mn orbitals with the Cr d-orbitals is considered. As shown in Fig. 7b, the e_g (t_{2g}) orbitals hybridize with the d_{z^2} , $d_{x^2-y^2}$ (d_{xy} , d_{yx} , d_{zx}) of Y atoms and form a lower energy bonding orbital e_g (t_{2g}) and a higher energy anti-bonding orbital e_g (t_{2g}). As Co and Mn atoms are in the center of a Y tetrahedron, the crystal field splitting of the bonding orbitals is $E(e_g) < E(t_{2g})$, and anti-bonding orbitals is $E(e_g) < E(t_{2g})$. Since t_{1u} , e_u cannot couple with any Y d-orbitals, the energy of $E(e_u) > E(t_{1u})$ is still remained. The complete hybridization orbitals of CoMnYZ are shown in Fig. 7c. The sp orbitals, the bonding orbitals e_g , and t_{2g} orbitals of CoMnYZ can jointly accommodate 18 valence electrons. The total number of valence electrons of CoMnYrZ ($Z = \text{Al, Ga, In}$) is 22, so there are still four valence electrons whose three electrons occupy the t_{1u} orbitals and one occupies the e_u orbitals of majority state, exclusively

localized at Co and Mn sites. Therefore, the Fermi level falls in the DOS of e_u of majority states and the gap is created between occupied (Co–Mn)–Y t_{12g} and unoccupied Co–Mn t_{1u} minority states. Thus, the minority electrons of CoMnYZ ($Z = \text{Al, Ga, In}$) present semiconductor character and the majority ones present metallic behavior, which causes these alloys to be half-metallic alloys. At the Fermi level, the spin-up DOS shows a metallic property, mainly due to Mn-d and this explains the large magnetic moment of Mn atom (Table 2).

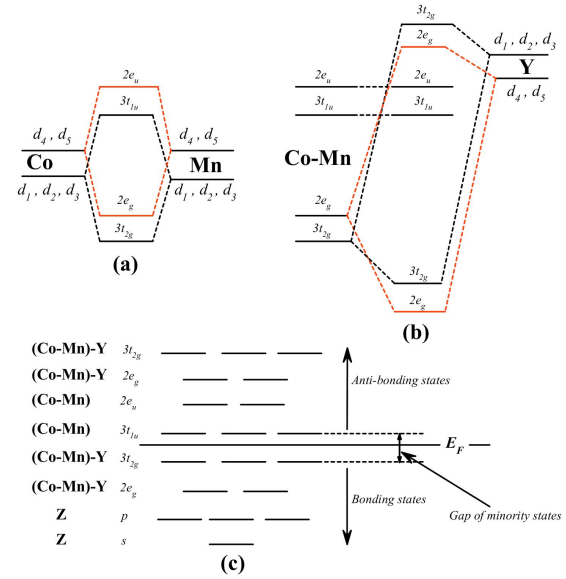


Fig. 7. Schematic illustration of the origin of the gap in the minority band in CoMnYZ alloy: d_1 , d_2 , d_3 , d_4 and d_5 denote the d_{xy} , d_{yx} , d_{zx} , d_{z^2} , $d_{x^2-y^2}$ orbitals, respectively.

Finally, the HM stability of CoMnYAl, CoMnYGa and CoMnYIn has been investigated under uniform strain and tetragonal distortion. Because HM materials are usually used in spintronic devices in the form of thin films or multilayers, the lattice constant will change when the thin films or multilayers are grown on appropriate substrates, and correspondingly, the half-metallicity may be destroyed. In order to study the effect of uniform strain (i.e. corresponding to hydrostatic pressure), we calculated the variation of valence band maximum (Max-VB) and conduction band minimum (Min-CB) as a function of lattice constant for

CoMnYAl, CoMnYGa and CoMnYIn plotted in Fig. 8a. It was found that the half-metallicity is kept in the wide range of 6.24 Å to 6.96 Å, 6.12 Å to 6.87 Å and 6.14 Å to 6.94 Å for CoMnYAl, CoMnYGa and CoMnYIn, respectively. Among these compounds the CoMnYIn has a considerable region of half-metallicity which makes it stable against negative and positive pressures. Moreover, in the CoMnYIn, the Fermi level is located in the middle of the minority band gap and therefore, this compound is the most stable compound against the effects which destroy the half-metallicity (such as temperature or external stresses). However, a common behavior in all CoMnYrZ (Z = Al, Ga, In) compounds is observed. With increasing the lattice constant, the minority valence band edge smoothly increases and subsequently cuts the Fermi level, while with decreasing the lattice constant the minority conduction band edge smoothly decreases and the half-metallicity disappears. Galanakis et al. [30] showed that the contraction and expansion of the lattice constant mainly influence the delocalized p electrons and do not affect the well localized d electrons of the transition metals considerably.

The effect of a tetragonal distortion with the c/a ratio, keeping the unit-cell volume the same as the equilibrium unit-cell volume, has been studied. The variations of valence band maximum (Max-VB) and conduction band minimum (Min-CB) as a function of c/a ratio for the CoMnYZ (Z = Al, Ga, In) compounds are shown in Fig. 8b. It can be seen that the CoMnYAl, CoMnYGa and CoMnYIn compounds show the half-metallic characteristics when c/a is in the range of 0.88 to 1.28, 0.88 to 1.26 and 0.83 to 1.31, respectively. The HM character sustains for relatively larger values of tetragonal strain. The (Min-CB) and (Max-VB) of minority spin channel are approximately maximum at the equilibrium lattice constant and the absolute value of them decreases monotonically with both positive and negative tetragonal strain. In a word, the considerable HM gaps and the robust half-metallicities under uniform and tetragonal strains make CoMnYAl, CoMnYGa and

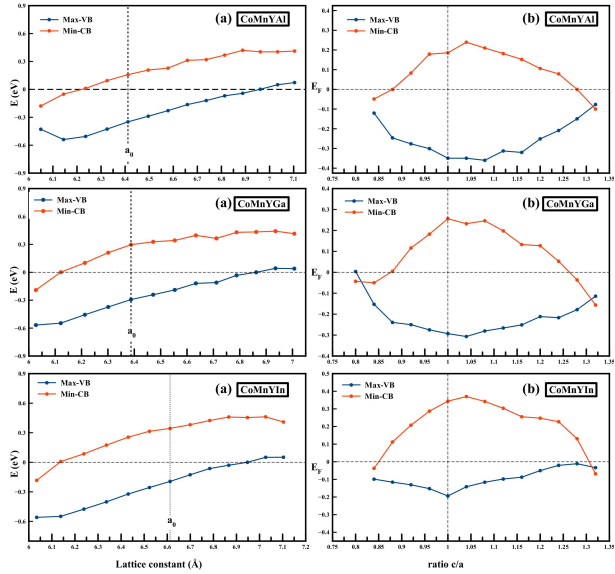


Fig. 8. Dependence of the HM state on the lattice constant (uniform strain) (a) and at the c/a ratio (tetragonal distortion) (b) of CoMnYZ (Z = Al, Ga, and In). The blue lines correspond to the valence bands maxima and the red lines correspond to the conduction band minima in the minority spin states (spin-down states).

CoMnYIn promising candidates for spintronic applications. As the equilibrium lattice constants of CoMnYAl, CoMnYGa and CoMnYIn compounds (6.4117 Å, 6.387 Å and 6.6122 Å, respectively) are close to that of zinc blende semiconductors such as InSb (6.48 Å) and CdTe (6.49 Å) [31], it is suggested to experimentally realize these HM Heusler alloys in the form of thin films on appropriate substrates and to use them as new candidates for applications in spintronic field.

The effect of the substitution of Z sp atoms on the structural, electronic and magnetic properties of CoMnYGa_{1-x}Al_x, CoMnYGa_{1-x}In_x and CoMnYAl_{1-x}In_x Heusler alloys has also been investigated. The calculated lattice constants a , semiconducting (spin-down) band gap E_g , half-metallic gap E_{HM} , total moment μ_{tot} and Curie temperature T_c at different compositions x are listed in Table 3, Table 4 and Table 5. The equilibrium lattice constants versus concentration are shown in Fig. 9, where our calculated lattice constants a have been found to vary almost linearly following Vegard's

law [32] with little marginal downward bowing parameters equal to 0.0122 Å for $\text{CoMnYGa}_{1-x}\text{Al}_x$, alloy obtained by adjusting the values calculated by a polynomial function. However, this systematic linear increase in the lattice parameter along the all series of alloys according to Vegard's law [32] suggests a good structural stability instead of forming a secondary phase. It has also been found that the values of the band gaps E_g are almost not affected by changing the concentration x (almost 0.5 eV). This behavior is consistent with previous works for other alloys such as $\text{Fe}_{3-x}\text{Mn}_x\text{Si}$ [33], $\text{Fe}_{3-x}\text{Cr}_x\text{Si}$ [34] and $\text{Fe}_2\text{Mn}_{1-x}\text{V}_x\text{Si}_{0.5}\text{Al}_{0.5}$ [35]. However, a little deviation of the band gap E_g from linear variation has been noticed. Fig. 10 shows the variation of the band gap E_g and half-metallic gap E_{HM} with concentration x in the $\text{CoMnYGa}_{1-x}\text{Al}_x$, $\text{CoMnYAl}_{1-x}\text{In}_x$ and $\text{CoMnYGa}_{1-x}\text{In}_x$ Heusler alloys. The second-order polynomial fitting of (E_g , E_{HM}) – x data gives the following equations for the three alloys :

$$E_g(x) = 0.3371x^2 - 0.4174x + 0.59(\text{CoMnYGa}_{1-x}\text{Al}_x) \quad (2)$$

$$E_g(x) = 0.3652x^2 - 0.3355x + 0.51(\text{CoMnYAl}_{1-x}\text{In}_x) \quad (3)$$

$$E_g(x) = 0.1971x^2 - 0.2473x + 0.59(\text{CoMnYGa}_{1-x}\text{In}_x) \quad (4)$$

and

$$E_{HM}(x) = 0.3168x^2 - 0.4529x + 0.294(\text{CoMnYGa}_{1-x}\text{Al}_x) \quad (5)$$

$$E_{HM}(x) = 0.2986x^2 - 0.2618x + 0.158(\text{CoMnYAl}_{1-x}\text{In}_x) \quad (6)$$

$$E_{HM}(x) = 0.1948x^2 - 0.2936x + 0.294(\text{CoMnYGa}_{1-x}\text{In}_x) \quad (7)$$

From the calculated results, the disorder is of the same order for all the alloys for E_g and E_{HM} ,

respectively. The half metallicity in the parent compounds CoMnYAl , CoMnYGa and CoMnYIn is also retained in all the alloys with the change of the concentration x of the doped Z atoms. The total magnetic moment is found to be integer ($4\mu_B$) for all alloys, in accordance with the Slater-Pauling rule. Curie temperature is another important aspect of application for spintronic material. Only with high Curie temperature can the magnetic materials be used in practice. Using the mean field approximation (MFA) [36], the Curie temperature (T_C) can be calculated as:

$$T_c = \frac{2\Delta E}{3k_B} \quad (8)$$

where ΔE is the total energy difference between the antiferromagnetic and ferromagnetic states ($\Delta E = E_{AFM} - E_{FM}$) and k_B is the Boltzmann constant. The results are given in Table 3, Table 4 and Table 5, and shown in Fig. 11. The Curie temperature has been calculated to be 482 K, 616 K and 805 K for CoMnYAl , CoMnYGa and CoMnYIn , respectively. It was also found that the Curie temperature significantly changes with Z content in all the three alloys $\text{CoMnYAl}_{1-x}\text{Ga}_x$, $\text{CoMnYGa}_{1-x}\text{In}_x$ and $\text{CoMnYAl}_{1-x}\text{In}_x$. The Curie temperature of the half-metallic Mn_2VAl compound, estimated by using the mean field approximation, is 638 K and its value is in good agreement with the experimental value of the Curie temperature of 760 K [37]. Also the results show that the Curie temperature of our half-metallic ferromagnetic doped alloys $\text{CoMnYAl}_{1-x}\text{Ga}_x$, $\text{CoMnYGa}_{1-x}\text{In}_x$ and $\text{CoMnYAl}_{1-x}\text{In}_x$ is higher than room temperature, so a wide range of scenarios can be acomodated. In addition, the Curie temperature increases almost proportionally with Z , with high valence-doped linearly. This behavior is consistent with previous theoretical works for alloys such as $\text{FeCoZrGe}_{1-x}\text{As}_x$ and $\text{FeCoZr}_{1-x}\text{Nb}_x\text{Ge}$ [38] and recent experimental studies on $\text{Co}_2\text{Ti}_{1-x}\text{Fe}_x\text{Ge}$ [39] and $\text{Co}_2\text{FeGa}_{1-x}\text{Si}_x$ [40] alloys.

4. Conclusions

In summary, the first-principles FPLAPW method based on DFT within the GGA has been

Table 3. Semiconducting gap E_g , half-metallic gap E_{HM} , total magnetic moment μ_{tot} and Curie temperature T_c of $CoMnYGa_{1-x}Al_x$ alloys.

x	a [Å]	E_g [eV]	E_{HM} [eV]	μ_{tot} [μ_B]	T_c [K]
0	6.387	0.59	0.294	4	616
0.25	6.3909	0.4886	0.176	4	593
0.5	6.3965	0.4763	0.157	4	553
0.75	6.4034	0.4693	0.14234	4	514
1	6.412	0.51	0.158	4	482

Table 4. Semiconducting gap E_g , half-metallic gap E_{HM} , total magnetic moment μ_{tot} and Curie temperature T_c of $CoMnYAl_{1-x}In_x$ alloys.

x	a [Å]	E_g [eV]	E_{HM} [eV]	μ_{tot} [μ_B]	T_c [K]
0	6.412	0.51	0.158	4	482
0.25	6.4652	0.43684	0.0993	4	610
0.5	6.5161	0.44	0.11	4	690
0.75	6.5641	0.4685	0.13	4	738
1	6.613	0.54	0.195	4	805

used to investigate the structural, elastic, electronic properties and magnetism of quaternary Heusler alloys of $CoMnYZ$ ($Z = Al, Ga, In$). In all the compounds, the stable Y-type 1+ FM structure was energetically more favorable than Y-type 2 and Y-type 3 structures. The negative formation energy indicates the thermodynamical stability of these alloys. The total magnetic moment M_{tot} in the unit cell is an integer of $4\mu_B$, which is following the Slater-Pauling rule $M_{tot} = (Z_{tot} - 18)$.

Table 5. Semiconducting gap E_g , half-metallic gap E_{HM} , total magnetic moment μ_{tot} and Curie temperature T_c of $CoMnYGa_{1-x}In_x$ alloys.

x	a [Å]	E_g [eV]	E_{HM} [eV]	μ_{tot} [μ_B]	T_c [K]
0	6.387	0.59	0.294	4	616
0.25	6.4403	0.54	0.23	4	690
0.5	6.497	0.5231	0.2	4	757
0.75	6.5508	0.505	0.18	4	774
1	6.613	0.54	0.195	4	805

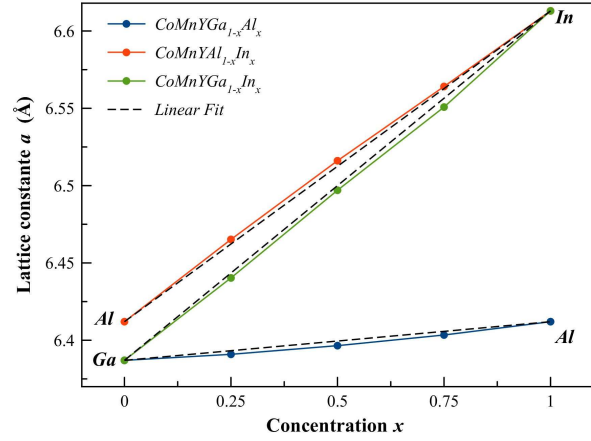


Fig. 9. The variation of the lattice parameter with concentration x of $CoMnYGa_{1-x}Al_x$, $CoMnYGa_{1-x}In_x$ and $CoMnYAl_{1-x}In_x$ Heusler alloys (dotted line is the linear fit).

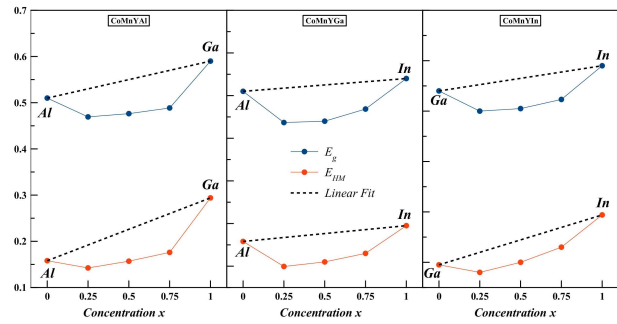


Fig. 10. Variation of the band gap E_g and half-metallic gap E_{HM} with concentration x of $CoMnYGa_{1-x}Al_x$, $CoMnYGa_{1-x}In_x$ and $CoMnYAl_{1-x}In_x$ Heusler alloys (dotted line is the linear fit).

The electronic structure calculations indicated that all the $CoMnYZ$ ($Z = Al, Ga, In$) compounds have HM characteristics with a large band gap in minority spin channel. This band gap was determined by the bonding (t_{2g}) and antibonding (t_{1u}) states created by the hybridizations of the d states of transition metal atoms Co, Mn and Y. The sensitivity of the half-metallicity was analyzed under hydrostatic distortion. The half-metallicity was robust for a wide range of lattice constants of 6.24 Å to 6.96 Å, 6.12 Å to 6.87 Å and 6.14 Å to 6.94 Å for Z elements of Al, Ga, and In, respectively. Furthermore, it was also revealed that $CoMnYZ$ ($Z = Al, Ga, In$) compounds are still HM under

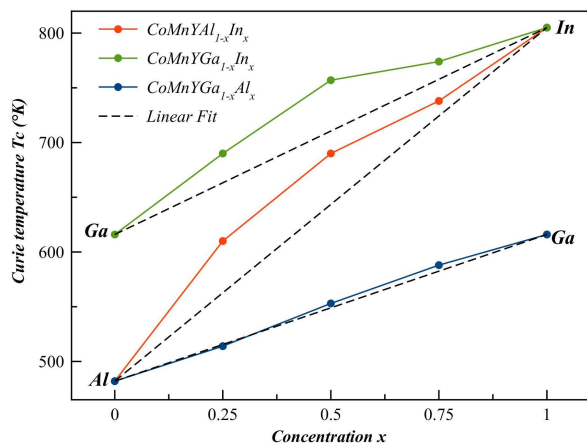


Fig. 11. Variation of Curie temperature with concentration x of $\text{CoMnYAl}_{1-x}\text{Ga}_x$, $\text{CoMnYGa}_{1-x}\text{In}_x$ and $\text{CoMnYAl}_{1-x}\text{In}_x$ Heusler alloys (dotted line is the linear fit).

appropriate tetragonal strains. Almost linear variation of the lattice constant and Curie temperature with x has been obtained. The band gap E_g and half-metallic gap E_{HM} exhibit non-linear behavior versus the composition x . Also the Curie temperature of our half-metallic ferromagnetic doped alloys $\text{CoMnYAl}_{1-x}\text{Ga}_x$, $\text{CoMnYGa}_{1-x}\text{In}_x$ and $\text{CoMnYAl}_{1-x}\text{In}_x$ is higher than room temperature. Therefore, we expect that our results would trigger further interest in incorporating these spin-filter materials (SFMs) as barriers in magnetic tunnel junction based devices.

References

- [1] GROOT DE R.A., MULLER F.M., ENGEN VAN P.G., BUSCHOW K.H.J., *Phys. Rev. Lett.*, 50 (1983), 2024.
- [2] GALANAKIS I., DEDERICHS P.H., PAPANIKOLAOU N., *Phys. Rev. B*, 17 (2002), 174429.
- [3] GALANAKIS I., MAVROPOULOS P., DEDERICHS P.H., *J. Phys. D Appl. Phys.*, 39 (2006), 765.
- [4] ŞASIOĞLU E., SANDRATSKI L.M., BRUNO P., GALANAKIS I., *Phys. Rev. B*, 72 (2005), 1844415.
- [5] SAITO T., KATAYAMA T., ISHIKAWA T., YAMAMOTO M., ASAKURA D., KOIDE T., MIURA Y., SHIRAI M., *Phys. Rev. B*, 81 (2010), 144417.
- [6] FARSHCHI R., RAMSTEINER M., *J. Appl. Phys.*, 113 (2013), 191101.
- [7] WEI X.P., DENG J.B., MAO G.Y., CHU S.B., HU X.R., *Intermetallics*, 29 (2012), 86.
- [8] KERVAN N., KERVAN S., *J. Magn. Magn. Mater.*, 324 (2012), 645.
- [9] KERVAN N., *J. Magn. Magn. Mater.*, 324 (2012), 4114.
- [10] DAI X., LIU G., FECHER G.H., FELSER C., LI Y., LIU H., *J. Appl. Phys.*, 105 (2009), 07E901.
- [11] XU G.Z., LIU E.K., DU Y., LI G.J., LIU G.D., WANG W.H., WU G.H., *EPL-Europhys. Lett.*, 102 (2013), 17007.
- [12] AL-ZYADI J.M.K., GAO G.Y., YAO K.L., *J. Magn. Magn. Mater.*, 378 (2015), 1.
- [13] FENG Y., CHEN H., YUAN H., ZHOU Y., CHEN X., *J. Magn. Magn. Mater.*, 378 (2015), 7.
- [14] BERRI S., MAOUCHE D., IBRIR M., ZERARGA F., *J. Magn. Magn. Mater.*, 354 (2014), 65.
- [15] KHODAMI M., AHMADIAN F., *J. Supercond. Nov. Magn.*, 28 (2015), 3027.
- [16] GAO Y.C., ZHANG Y., WANG X.T., *J. Korean Phys. Soc.*, 66 (2015), 959.
- [17] KLAER P., BALKE B., ALIJANI V., WINTERLIK J., FECHER G.H., FELSER C., ELMERS H.J., *Phys. Rev. B*, 84 (2011), 144413.
- [18] ALIJANI V., WINTERLIK J., FECHER G.H., NAGHAVI S.S., FELSER C., *Phys. Rev. B*, 83 (2011), 184428.
- [19] ALIJANI V., OUARDI S., FECHER G.H., WINTERLIK J., NAGHAVI S.S., KOZINA X., STRYGANYUK G., FELSER C., IKENAGA E., YAMASHITA Y., UEDA S., KOBAYASHI K., *Phys. Rev. B*, 84 (2011), 224416.
- [20] GORIPATI H.S., FURUBAYASHI T., TAKAHASHI Y.K., HONO K., *J. Appl. Phys.*, 113 (2013), 043901.
- [21] HOHENBERG P., KOHN W., *Phys. Rev.*, 136 (1964), B864.
- [22] JANSEN H.J.F., FREEMAN A.J., *Phys. Rev. B*, 30 (1984), 561.
- [23] BLAHA P., SCHWARZ K., MADSEN G.K.H., KVASNICKA D., LUITZ J., WIEN2k, *An Augmented Plane Wave + Local Orbitals Program for Calculating Crystal Properties*, Technische Universität Wien, Austria, 2001.
- [24] PERDEW J.P., BURKE S., ERNZERHOF M., *Phys. Rev. Lett.*, 77 (1996), 3865.
- [25] MURNAGHAN F.D., *P. Natl. Acad. Sci. USA* 30 (1944), 5390.
- [26] LIU Y., BOSE S.K., KUDRNOVSKÝ J., *Phys. Rev. B*, 82 (2010), 094435.
- [27] GALANAKIS I., MAVROPOULOS P., *Phys. Rev. B*, 67 (2003), 104417.
- [28] GRAF T., FELSLER C., PARKIN S.P.P., *Prog. Solid State Ch.*, 39 (2011), 1.
- [29] WEI X.P., DENG J.B., MAO G.Y., CHU S.B., HU X.R., *Intermetallics*, 29 (2012), 86.
- [30] GALANAKIS I., ÖZDOĞAN K., ŞASIOĞLU E., *J. Phys.-Condens. Mat.*, 26 (2014), 086003.
- [31] MADELUNG O., (Ed.), *Physics of II VI and I VII Compounds, Semimagnetic Semiconductors / Physik der II VI und I VII-Verbindungen, semimagnetische Halbleiter Elemente*, Vol. 17b, Springer-Verlag, Berlin Heidelberg, 1982.
- [32] VEGARD L., *Z. Phys. Chem.*, 5 (1921), 17.
- [33] HAMAD B., KHALIFEH J., ADU ALJARAYESH I., DEMANGEAT C., LUO H.B., HU Q.M., *J. Appl. Phys.*, 107 (2010), 09311.

- [34] HAMAD B., KHALIFEH J., HU Q.M., DEMANGEAT C., *J. Mater. Sci.*, 47 (2012), 797.
- [35] HAMAD B., CHARIFI Z., BAAZIZ H., SOYALP F., *J. Magn. Magn. Mater.*, 324 (2012), 3345.
- [36] SATO K., DEDERICHS P.H., KATAYAMA-YOSHIDA H., KUDRNOVSKY J., *J. Phys.:Condens. Matter.*, 16 (2004), S5491.
- [37] ŞASIOĞLU E., SANDRATSKII L.M., BRUNO P., *J. Phys.-Condens. Mat.*, 17 (2005), 995.
- [38] MAO G.-Y., LIU X.-X., GAO Q., LI L., XIE H.-H., LEI G., DENG J.-B., *J. Magn. Magn. Mater.*, 398 (2016), 1.
- [39] VENKATESWARLU B., MIDHUNLAL P.V., BABU P.D., HARISH KUMAR N., *J. Magn. Magn. Mater.*, 407 (2016), 142.
- [40] DEKAN B., CHAKRABORTY D., SRINIVASAN A., *Physica B*, 448 (2014), 173.

Received 2016-05-24

Accepted 2016-10-19